Study of the Reaction $C^{12}(d, p)C^{13}$ with the Weakly-Bound-Projectile Model*

C. A. PEARSON AND J. C. WILCOTT
Department of Physics, University of Arizona, Tucson, Arizona 85721
(Received 5 September 1968)

Predictions of the weakly-bound-projectile model are compared with measured differential cross sections, polarization, and vector-analyzing power for the reactions $C^{12}(d, p)C^{13}$(g.s.) at deuteron energies between 7.0 and 26 MeV, and $C^{12}(d, p)C^{13*}$(3.09 MeV) between 10 and 15 MeV. All the measurements are accounted for without any compound-nucleus resonance effects. It is suggested that previous failures to fit such data with the distorted-wave Born approximation stem from its inadequate description of the stripping mechanism.

I. INTRODUCTION

THE reaction $C^{12}(d, p)C^{13}$ was one of the first stripping reactions to be studied.[1,2] Many measurements have since been made.[3–22] Most of them have yet to be explained.

Although the reaction shows many of the features of a direct reaction, attempts to fit the data with conventional distorted-wave Born-approximation (DWBA) calculations have consistently failed. Several angular distributions have been calculated[8,22–24] for the reactions $C^{12}(d, p)C^{13}$(g.s.), $l_n=1$, $j_n=\frac{1}{2}$, and $C^{12}(d, p)C^{13*}$(3.09 MeV), $l_n=0$. Widely different parameters were used for each case. The detailed behavior of the measured angular distributions has not been reproduced. At certain angles the calculated and measured cross sections differ from each other by an order of magnitude, and the positions of maxima and minima are often incorrect.

The angle dependence of outgoing proton polarization has been measured at various bombarding energies for the same reactions. DWBA calculations have failed to reproduce the qualitative behavior of this polarization at any energy.[9,25,26]

Recently, polarized deuteron beams have been used to initiate these reactions and the angle dependence of the vector analyzing power has been accurately measured at several energies.[20–22] Attempts to fit these measurements with DWBA calculations have also failed.[22]

To account for the disagreement, it has been suggested that compound-nucleus resonance effects which are known to be present at low bombarding energies[27,28] also occur at higher energies,[8,22] even up to 22 MeV.[9] Then the DWBA, which represents only the direct reaction stripping amplitude, is not expected to fit the measurements.

Without substantial resonance effects the disagreement implies either that the search for parameters has not been sufficiently comprehensive, or that the DWBA is an inadequate description of the reaction mechanism. The latter conclusion is likely.

The DWBA represents the weak deuteron structure as undisturbed on sudden impact with the target nucleus, the whole structure being deflected by a force acting on its c.m. Because the deuteron is similar to the C^{12} nucleus in size, at impact only one of its component nucleons will usually be interacting at a time. This will tend to tear the deuteron apart, and the DWBA description seems particularly inappropriate.

An approximate three-body model, the weakly-bound-projectile (WBP) model, has been recently

* Work supported in part by NSF Grant No. GU-1534.

[1] J. Rotblat, Phys. Rev. **83**, 1271 (1951); Nature **167**, 1027 (1951); E. J. Burge, H. B. Burrows, W. M. Gibson, and J. Rotblat, Proc. Roy. Soc. (London) **A210**, 534 (1951).

[2] S. T. Butler, Proc. Roy. Soc. (London) **A208**, 559 (1951); A. B. Bhatia, K. Huang, R. Huby, and H. C. Newns, Phil. Mag. **43**, 485 (1952).

[3] R. J. Slobodrian, Phys. Rev. **126**, 1059 (1962).

[4] N. Zaika, O. F. Nemets, and S. Tserino, Zh. Eksperim. i Teor. Fiz. **39**, 1 (1960) [English transl.: Soviet Phys.—JETP **12**, 1 (1960)].

[5] E. W. Hamburger, Phys. Rev. **123**, 619 (1961).

[6] S. Morita, N. Kawai, N. Takano, Y. Goto, R. Hanada, Y. Nakajima, S. Takemoto, and Y. Yaegashi, J. Phys. Soc. Japan **15**, 550 (1960).

[7] U. Schmidt-Rohr, R. Stock, and P. Turek, Nucl. Phys. **53**, 77 (1964).

[8] J. P. Schiffer, G. C. Morrison, R. H. Siemssen, and B. Zeidman, Phys. Rev. **164**, 1274 (1967).

[9] J. E. Evans, J. A. Kuehner, and E. Almqvist, Phys. Rev. **131**, 1632 (1963).

[10] R. W. Bercaw and F. B. Shull, Phys. Rev. **133B**, 632 (1964).

[11] R. Van Dantzig and L. A. ch. Koerts, Nucl. Phys. **48**, 177 (1963).

[12] B. Hird, J. Cookson, and M. S. Bokhari, Proc. Phys. Soc. (London) **72**, 489 (1958); M. S. Bokhari, J. A. Cookson, B. Hird, and B. Wessakul, *ibid.* **72**, 88 (1958).

[13] R. G. Allas and F. B. Shull, Phys. Rev. **116**, 996 (1959).

[14] W. P. Johnson and D. W. Miller, Phys. Rev. **124**, 1190 (1961).

[15] A. C. Juveland and W. Jentschke, Phys. Rev. **110**, 456 (1958).

[16] A. Isoya, S. Micheletti, and L. H. Reber, Phys. Rev. **128**, 806 (1962).

[17] L. H. Reber and J. X. Saladin, Phys. Rev. **133**, B1155 (1964).

[18] R. Beurtey, R. Chaminade, A. Falcoz, R. Maillard, T. Mikumo, A. Papineau, L. Schecter, and J. Thirion, J. Phys. Paris **24**, 1038 (1963).

[19] E. T. Boschitz, in *Proceedings of the Conference on Direct Interactions and Nuclear Reaction Mechanisms Padua, 1962*, edited by E. Clementel and C. Villi (Gordon and Breach, Science Publishers, Inc., New York, 1963), p. 642.

[20] A. M. Baxter, J. A. R. Griffith, and S. Roman, Phys. Rev. Letters **20**, 1114 (1968).

[21] T. J. Yule and W. Haeberli, Phys. Rev. Letters **19**, 756 (1967).

[22] T. J. Yule and W. Haeberli, Nucl. Phys. **A117**, 1 (1968).

[23] R. van Dantzig and W. Tobocman, Phys. Rev. **136**, B1682 (1964).

[24] W. R. Smith and E. V. Ivash, Phys. Rev. **131**, 304 (1963).

[25] D. Robson, Nucl. Phys. **22**, 34 (1961).

[26] N. S. Chant, P. S. Fisher, and D. K. Scott, Nucl. Phys. **A99**, 669 (1967).

[27] M. T. McEllistrem, K. W. Jones, Ren Chiba, R. A. Douglas, D. F. Herring, and E. A. Silverstein, Phys. Rev. **104**, 1008 (1956).

[28] A. Elwyn, J. V. Kane, S. Ofer, and D. H. Wilkinson, Phys. Rev. **116**, 1490 (1959).

TABLE I. Average nucleon-nucleus parameters of Rosen *et al.* (see Ref. 33).

	Neutron	Proton
V (MeV)	$49.3-0.33E$	$53.8-0.33E$
W (MeV)	5.75	7.5
R (fm)	$1.25A^{1/3}$	$1.25A^{1/3}$
a (fm)	0.65	0.65
b(fm)	0.70	0.70
V_s (MeV)	5.5	5.5

proposed by Pearson and Coz[29,30] to avoid the difficulties inherent in the DWBA concept. Preliminary calculations with the model account for the shape and magnitude[31] as well as the j_n dependence[32] of measured differential cross sections. The same calculations reproduce the qualitative behavior of measured polarization over a range of energy, angular momentum transfer and target nuclei.[31]

It is particularly interesting to apply the WBP model to the reaction $C^{12}(d, p)C^{13}$, to test the WBP mechanism, to look for resonance effects, and to evaluate the DWBA.

In this paper, we report calculations for the reaction $C^{12}(d, p)C^{13}$(g.s.)$l_n=1$, $j_n=\frac{1}{2}$, at incident energies between 7 and 26 MeV, and for the reaction $C^{12}(d, p)C^{13*}$(3.09 MeV), $l_n=0$, between 10 and 15 MeV.

These calculations use the standard nucleon-nucleus optical-model parameters of Rosen *et al.*[33] except for a radius change which improves the fit to elastic scattering polarization.[33]

We find that the angle dependence of the differential cross section, polarization, and vector-analyzing power are accounted for at all energies without resonant contributions. Our results are consistent with a small isotropic compound-nucleus background which may range in magnitude from 0.5 mb/sr at deuteron energies of 12 MeV to 0.025 mb/sr at 26 MeV.

The calculations reported here not only confirm the basic mechanism of the WBP model; they suggest that the failure of previous DWBA calculations stems from an inappropriate description of the direct reaction stripping mechanism. In Sec. II, we present relevant formulas. In Sec. III, we compare our calculations with experiment. In Sec. IV, we discuss some qualitative features of the calculations and the source of small anomalies. In Sec. V, we present conclusions.

[29] C. A. Pearson and M. Coz, Nucl. Phys. **82**, 533 (1966); **82**, 545 (1966).
[30] C. A. Pearson and M. Cozl, Ann. Phys. (N.Y.) **39**, 199 (1966).
[31] C. A. Pearson, L. Pocs, and J. M. Bang, Ann. Phys. (N.Y.) **52**, 33 (1969).
[32] C. A. Pearson, L. Pocs, and J. M. Bang (unpublished).
[33] L. Rosen, J. G. Beery, A. S. Goldhaber, and E. H. Auerbach, Ann. Phys. (N.Y.) **34**, 96 (1965).

II. CALCULATION

In our calculations, we make the usual assumption that the neutron is deposited in a single-particle orbit around the unexcited spin-zero target nucleus core. As frame of reference we choose the barycentric frame with the z axis along $\mathbf{k}_d$ and the y axis in the direction $\mathbf{k}_d\times\hat{\mathbf{k}}_p$.

With notation similar to Refs. 30–32 and 34 the WBP amplitude is

$$T_{\mu_d\mu_p M_n}=\sum_{\mu_{p'}}\langle\tfrac{1}{2}\,\mu_{p'}\,\tfrac{1}{2}\,\mu_{n'}\mid 1\,\mu_d\rangle \times(4\pi)^{1/2}N\int d\mathbf{k}_{p'}\left[\frac{1}{K^2+\gamma^2}-\frac{1}{K^2+\zeta^2}\right]\mathcal{S}_{\mu_{p'}\mu_p}(\mathbf{k}_{p'},\mathbf{k}_p) \times\langle v(\mathbf{r}_n)\mid\mathcal{U}(\mathbf{r}_n,\mathbf{k}_{p'})\mid u_{\mu_n'}{}^{+}(\mathbf{r}_n,\mathbf{k}_{n'})\rangle. \quad (1)$$

It is convenient to substitute for the proton scattering matrix

$$\mathcal{S}_{\mu_{p'}\mu_p}(\mathbf{k}_{p'},\mathbf{k}_p)=\delta_{\mu_{p'}\mu_p}\delta(\mathbf{k}_{p'}-\mathbf{k}_p) -2\pi i\delta(E_{p'}-E_p)T_{\mu_{p'}\mu_p}(\mathbf{k}_{p'},\mathbf{k}_p) \quad (2)$$

so that the amplitude (1) becomes a sum of two terms. In keeping with previous nomenclature[31–32,34] we call these the "unscattered" and "scattered" amplitudes, respectively. The "unscattered" amplitude corresponds to just the plane-wave part of the proton S matrix.

The method of evaluating (1) has been described in detail in Refs. 31 and 32. We use the same approximations as in previous calculations.[31–32] The zero-range approximation for the neutron-proton interaction V_{np} is made in the neutron-capturing interaction

$$\mathcal{U}(\mathbf{r}_n,\mathbf{k}_{p'})=\int\mid\chi_p{}^{+}(\mathbf{k}_{p'},\mathbf{r}_p)\mid^2 V_{np}(\mathbf{r}_n-\mathbf{r}_p)\,d\mathbf{r}_p, \quad (3)$$

which is replaced by

$$\mathcal{U}(\mathbf{r}_n,\mathbf{k}_{p'})=-(\hbar^2/m)(K^2+\gamma^2)\mid\chi_p{}^{+}(\mathbf{r}_n,\mathbf{k}_{p'})\mid^2 \quad (4)$$

with $\mathbf{K}=\frac{1}{2}\mathbf{k}_d-\mathbf{k}_p$. The bound-neutron wave function is evaluated in a local Woods-Saxon potential, and contributions from the d-state component of the deuteron are neglected.

These approximations overemphasize contributions from the nuclear interior and reduce the magnitude of predicted cross sections.[34] However, they have little effect on the angle dependence of the polarization, vector-analyzing power, and differential cross sections which depend most strongly on the proton scattering.[34,35]

In terms of the amplitude (1), the differential cross section is

$$\frac{d\sigma}{d\Omega}=\frac{1}{3}\left(\frac{1}{2\pi\hbar^2}\right)^2 m_p{}^{*}m_d{}^{*}\frac{k_d}{k_p}\sum_{\mu_d\mu_p M_n}\mid T_{\mu_d\mu_p M_n}\mid^2, \quad (5)$$

[34] J. M. Bang and C. A. Pearson, Nucl. Phys. **A100**, 1 (1967); J. M. Bang, C. A. Pearson, and L. Pocs, *ibid.* **A100**, 24 (1967).
[35] C. A. Pearson, J. C. Wilcott, and L. C. McIntyre, Nucl. Phys. **A125**, 111 (1969).

and the polarization

$$P_y = \frac{-2\,\mathrm{Im}\sum_{\mu_d M_n} T_{\mu_d \frac{1}{2} M_n} T_{\mu_d -\frac{1}{2} M_n}^*}{\sum_{\mu_d \mu_p M_n} |T_{\mu_d \mu_p M_n}|^2}. \quad (6)$$

The vector-analyzing power P_d, measured with a polarized deuteron beam, is defined in Refs. 21 and 22,

$$P_d(\theta) = (1/3p)\{[\sigma_{\mathrm{up}}(\theta) - \sigma_{\mathrm{down}}(\theta)]/\sigma_{\mathrm{unp}}(\theta)\}, \quad (7)$$

where p is the vector polarization of the incident beam, σ_{up} and σ_{down} are cross sections measured with the deuteron spins up and down, respectively, parallel and antiparallel to our y axis, and σ_{unp} is the corresponding cross section with the incident beam unpolarized. In terms of the amplitude (1), P_d is

$$P_d = \frac{+2^{1/2}\,\mathrm{Im}\sum_{\mu_p M_n}[T_{0\mu_p M_n} T_{-1\mu_p M_n}^* + T_{1\mu_p M_n} T_{0\mu_p M_n}^*]}{\sum_{\mu_d \mu_p M_n} |T_{\mu_d \mu_p M_n}|^2}. \quad (8)$$

In Refs. 21 and 22, the quantity

$$P_d^1(\theta) = \frac{2}{3p}\left[\frac{\sigma_{\mathrm{up}}(\theta) - \sigma_{\mathrm{down}}(\theta)}{\sigma_{\mathrm{up}}(\theta) + \sigma_{\mathrm{down}}(\theta)}\right], \quad (9)$$

which differs from (7) through contributions from tensor polarization of the incident deuteron beam, was measured. It was suggested that

$$R = |(P_d^1 - P_d)/P_d| \lesssim 0.035. \quad (10)$$

We have calculated the quantity (10) at each angle using the magnitudes[22]

$$p_z = 0.274$$

and

$$p_{zz} = 0.293$$

for the vector and tensor polarization. In isolated cases at large angles, we find $R \approx 0.2$, but usually $R \leq 0.035$.

III. COMPARISON WITH EXPERIMENT

A. Parameters

The bound-state wave function was calculated as previously described.[34] For the scattered wave functions, the nucleon-nucleus optical potentials had the form

$$V(r) = -Vf(r) - iWg(r) - V_s h(r)\boldsymbol{\sigma}\cdot\mathbf{l} + V_c(r), \quad (11)$$

where

$$f(r) = \{1+\exp[(r-R)/a]\}^{-1}, \qquad R = r_0 A^{1/3}$$

$$g(r) = -4b(d/dr)\{1+\exp[(r-R)/b]\}^{-1}(1-s) + 4s/\{1+\exp[(r-R)/b]\},$$

$$h(r) = -\lambda_\pi^2 (1/r)(df/dr).$$

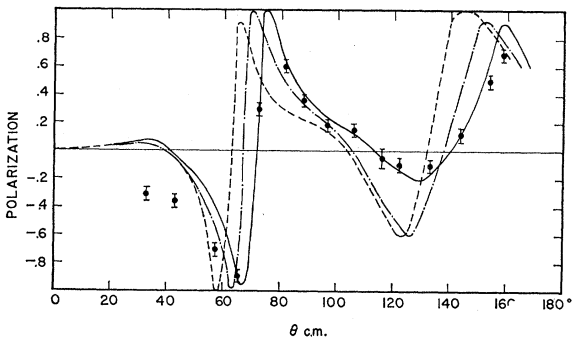

FIG. 1. Calculated and measured proton polarization for elastic scattering from C^{12}, $E_p = 14.5$ MeV. Measurements from Ref. 33. Calculations use potential of Sec. III, parameters from Ref. 33 with $r_0 = 1.25$ (broken curve), 1.15 (broken-dotted curve), and 1.05 (solid curve).

The proton potential was truncated as in Refs. 31–32 and 34.

It was initially intended to report the predictions of the WBP model for the reaction $C^{12}(d, p)C^{13}$, using the average nucleon-nucleus parameters of Rosen *et al.*[33] The Rosen parameters are given in Table I. However, in the case of C^{12} the average optical-model parameters of Ref. 33 give a poor fit to the elastic scattering data. A change to smaller radius is indicated. Smaller radii have also been found for proton scattering from C^{12} by other authors.[36,37]

In Fig. 1, we show the improvement in fitting proton polarization in elastic scattering from C^{12} at $E_p = 14.5$ MeV,[33] when the radius of our proton potential is changed to $R = 1.15\,A^{1/3}$ and $R = 1.05\,A^{1/3}$, respectively. The remaining parameters are from Ref. 33. The smallest radius clearly gives the best fit.

In the present work, we report calculations with three different parameter sets to emphasize that reasonable changes in parameters do not change the qualitative nature of the predictions. It is not necessary to use different sets to reproduce the data. Fits using set C are equivalent to any shown. We list only the parameters which differ from the average parameters of Ref. 33:

set A: $W_n = 8$ MeV, $s_n = 0.33$, $R_n = R_p = 1.15A^{1/3}$;

set B: $R_n = R_p = 1.05\,A^{1/3}$;

set C: $R_n = 1.15\,A^{1/3}$, $R_p = 1.05\,A^{1/3}$.

The $C^{12}(d, p)C^{13}$(g.s.) calculations were performed first. Set A parameters were used, the choice for W_n being the same as for the polarization calculations of Ref. 31. However, the reaction $C^{12}(d, p)C^{13*}$(3.09 MeV) with l_n zero is more sensitive to R_p in a manner similar to elastic scattering.[29–32,34] Both this reaction and the elastic scattering polarization of Fig. 1 require $R_p = 1.05A^{1/3}$, and set B parameters were used. Set C provides a suitable compromise.

[36] G. R. Satchler, Nucl. Phys. **85**, 273 (1966).
[37] M. Fricke and G. R. Satchler, Phys. Rev. **139**, B567 (1965).

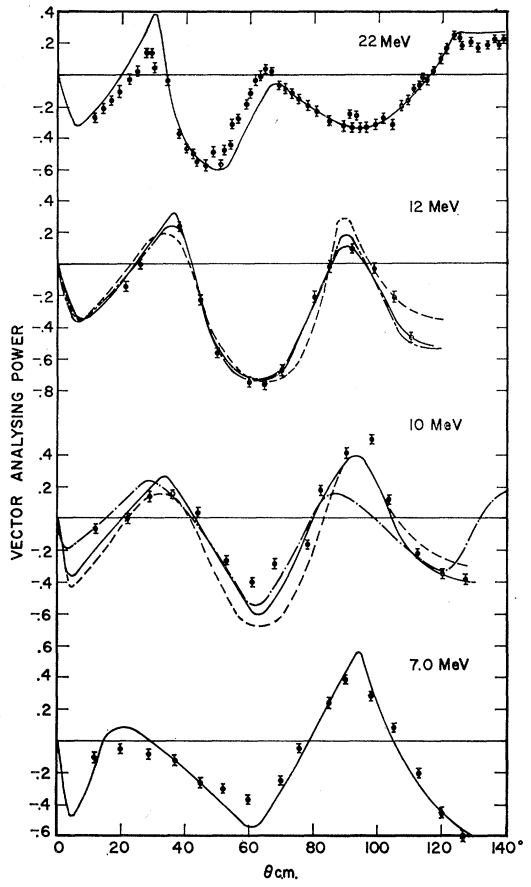

FIG. 2. Calculated and measured P_d for reaction $C^{12}(d, p)C^{13}$-(g.s.). Measurements from Ref. 22 (7.0 and 10 MeV), Ref. 20 (11.9 MeV), and Ref. 18 (22 MeV). Solid curves use set A parameters, broken curves set C, and broken-dotted curves set A with $W_n=11$ MeV, $s=0.0$ ($E_d=12$ MeV), set A with $W_n=W_p=3$ MeV, $s=0.0$ ($E_d=10$ MeV).

B. Detailed Comparison

In Fig. 2, we compare calculated and measured values for P_d in the reaction $C^{12}(d, p)C^{13}$(g.s.) at deuteron energies between 7 and 22 MeV. Solid curves are calculated with set A parameters, broken curves with set C, and the dotted-broken curve at 11.9 MeV with set A except that $W_n=11$ MeV, $s=0.0$ is used for the neutron absorption. All these parameters give similar results. The calculated values for P_d are not sensitive to details of the neutron absorption.

In Fig. 3, we make similar comparisons between calculated and measured values for the proton polarization P_y with unpolarized incident deuterons. Solid curves are calculated with set A parameters, the broken curve at 10.0 MeV with set C. Set A and set C parameters give similar results. The main disagreement with the data is near 30° where the calculated and measured polarization differ in sign, and at higher energies near 80°.

In comparing Fig. 3 and Fig. 2, one notes the qualitative similarity in the angle dependence for P_d and P_y. However, in general, there is no simple quantitative relationship as proposed in Ref. 20. We show in Sec. IV that P_y is much more sensitive to the spin-orbit force on the proton than P_d. When this force is zero, P_d and P_y are related by (14).

In Figs. 4–6, we compare calculated and measured angular distributions for the reaction $C^{12}(d, p)C^{13}$(g.s.) at deuteron energies between 7 and 26 MeV.

The data in Fig. 4 are displayed on a linear scale as in Refs. 4 and 5. The calculations reproduce the positions of maxima and minima at all energies. At large angles, the calculated curves are smaller than the measured values, the discrepancy decreasing as the energy increases.

It is possible that an unpolarized compound nucleus background accounts for the difference.[9,27,28] Measurements of polarization[9] and P_d[22] near 8 MeV for the reaction $C^{12}(d, p)C^{13*}$(3.09 MeV) are sensitive to small variations in deuteron energy, suggesting compound-nucleus resonance effects. However, the fits to P_d at

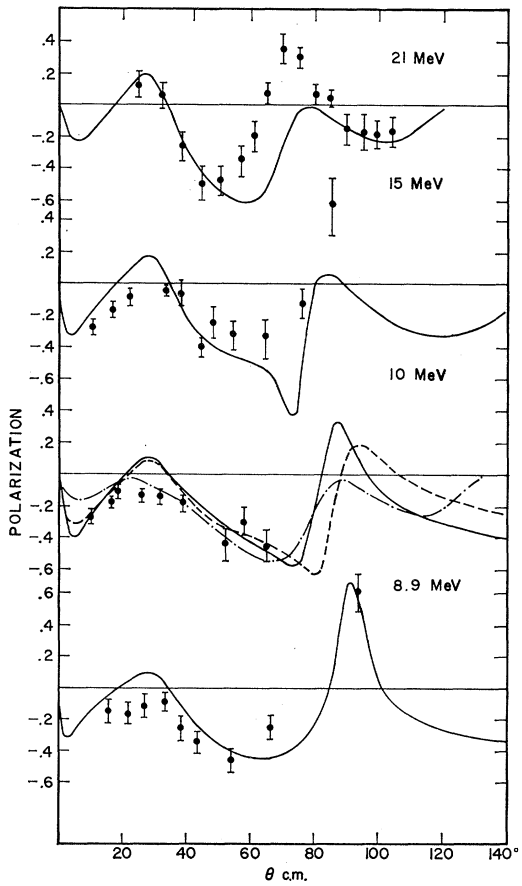

FIG. 3. Calculated and measured P_y for reaction $C^{12}(d, p)C^{13}$-(g.s.). Measurements from Ref. 12 (8.9 MeV), Ref. 10 (10.0 MeV), Ref. 14 (10.8 MeV), Ref. 16 (15 MeV), and Ref. 19 (21 MeV). Solid curves use set A parameters, broken curve set C, broken-dotted curve set A with $W_n=W_p=3$ MeV, $s=0.0$.

7 MeV in Fig. 2, and P_y at 8.9 MeV in Fig. 3 do not indicate such effects.

On the other hand, the discrepancy may lie within experimental error. The difference between measured

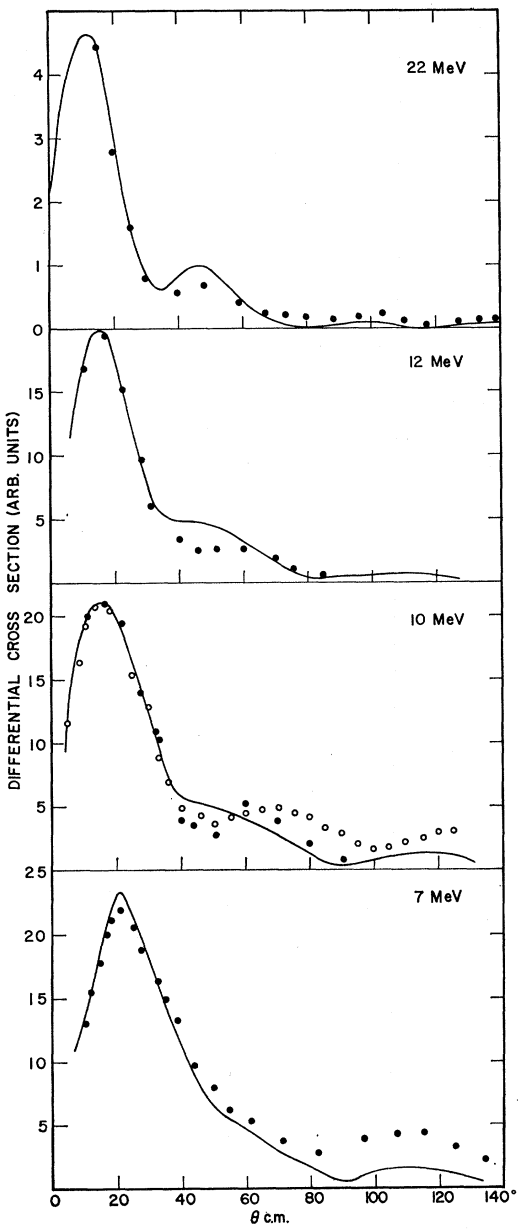

FIG. 4. Calculated and measured angular distributions for the reaction $C^{12}(d, p)C^{13}$(g.s.). Measurements are from Ref. 4 (7.15 and 9.6 MeV), Ref. 5 (10.2 and 12.4 MeV), and Ref. 6 (19.6 MeV). Solid curves are calculated with set A parameters at indicated energies.

curves at 9.6 and 10.2 MeV (Refs. 4, 5) is the same order as the difference between the calculated and measured curves.

Comparison with more recent experimental data is made in Figs. 5 and 6. Solid curves include constant

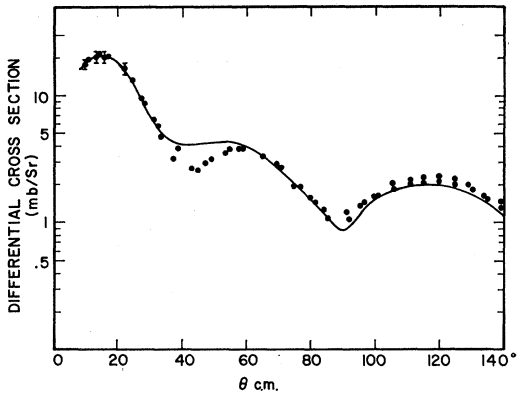

FIG. 5. Calculated and measured angular distributions for the reaction $C^{12}(d, p)C^{13}$(g.s.). Measurements are from Ref. 8 (12.0 MeV), and Ref. 7 (11.8 MeV). Solid curve is calculated with set A parameters (E_d=11.9 MeV) and includes uniform background of 0.5 mb/sr.

background contributions of 0.5 mb/sr (E_d=12 MeV) and 0.025 mb/sr (E_d=26 MeV). This background contribution represents the amount by which curves calculated with set A parameters fall below the last maximum in the measured angular distribution. The curves for P_d and P_y in Figs. 2 and 3 would be qualitatively unchanged by such unpolarized backgrounds.

In Figs. 7 and 8, we compare calculated and measured values for P_d, P_y, and differential cross sections for the reaction $C^{12}(d, p)C^{13*}$(3.09 MeV) (with l_n=0, j_n=$\frac{1}{2}$) at deuteron energies between 10 and 15 MeV. Solid curves are calculated with set B parameters, the dashed curve at 11.9 MeV with set C.

Sets B and C give similar results. The main disagreement with the data is near 70° in the poorly measured 15-MeV polarization. The calculated minimum in P_d dna P_y near 30° is too small.

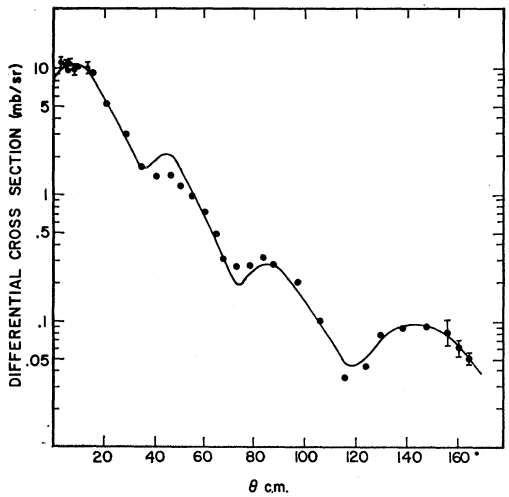

FIG. 6. Calculated and measured angular distributions for reaction $C^{12}(d, p)C^{13}$(g.s.) (E_d=26 MeV). Measurements are from Ref. 11. Solid curve is calculated with set A parameters, and includes uniform background of 0.025 mb/sr.

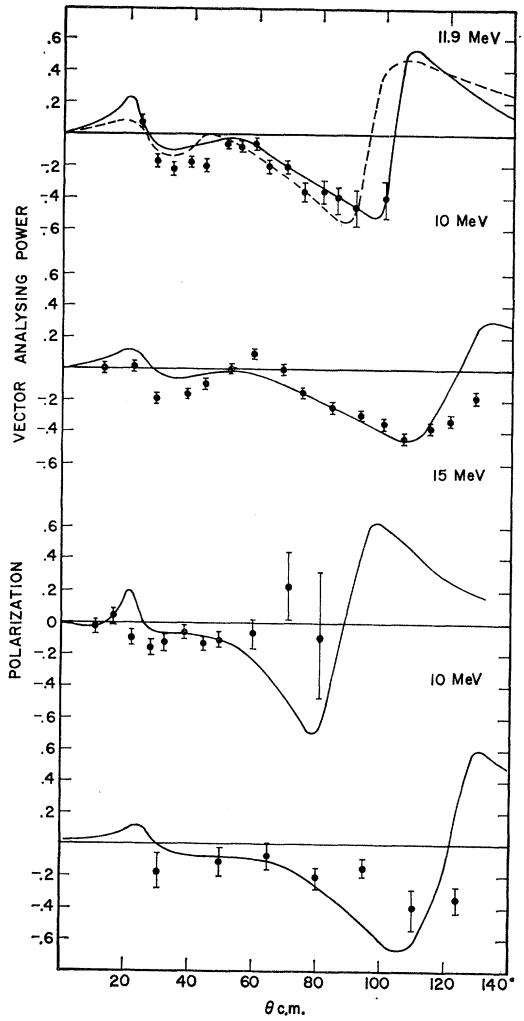

FIG. 7. Calculated and measured values for P_d, P_y for reaction $C^{12}(d, p)C^{13*}(3.09\ \text{MeV})$ ($l_n=0$, $j_n=\frac{1}{2}$). Polarization measurements are from Ref. 9 (10 MeV) and Ref. 17 (15 MeV). Measured values for P_d are from Ref. 22 (10 MeV) and Ref. 20 (11.9 MeV). Solid curves are calculated with set B parameters, dashed curve at 11.9 MeV with set C.

We emphasize that the curves shown above do not represent best fits. It should certainly be possible to find a single set of parameters which fit the data better than the calculations we have shown. However, such detailed parameter searches are usually meaningless. Often interesting anomalies are concealed by slightly unphysical choice of parameters.

In Fig. 9, we compare the DWBA calculations of Ref. 22 with measurements for P_d for the two reactions $C^{12}(d, p)C^{13}$(g.s.) and $C^{12}(d, p)C^{13*}$ (3.09 MeV), at deuteron energy 10.0 MeV. The calculated curves bear no relation to the data.

IV. QUALITATIVE PROPERTIES AND ANOMALIES

A. Qualitative Properties

In the WBP model, the neutron and proton play separate roles. Some features of P_d and P_y are determined mainly by the neutron capture, others by the proton scattering. We discuss certain qualitative properties of the model before returning to the anomalies.

1. *Reactions with* $l_n=0$

When the neutron scattering potential contains no spin-orbit term, the capture factor

$$\langle v_{M_n}(\mathbf{r}_n) \mid \mathcal{U}(\mathbf{r}_n, \mathbf{k}_{p'}) \mid u_{\mu_{n'}}{}^{+}(\mathbf{r}_n \mathbf{k}_{n'}) \rangle$$

in (1) is zero if $M_n \neq \mu_{n'}$. When the proton potential also contains no spin-orbit term the amplitude (1) has the form

$$T_{\mu_d \mu_p M_n} = \langle \tfrac{1}{2}\, \mu_p\, \tfrac{1}{2}\, M_n \mid 1\, \mu_d \rangle A, \qquad (12)$$

where A does not depend on M_n, μ_p, and P_d, P_y both vanish. In reactions with $l_n=0$, P_d, P_y thus stem from spin dependence of the distorted waves. Calculations

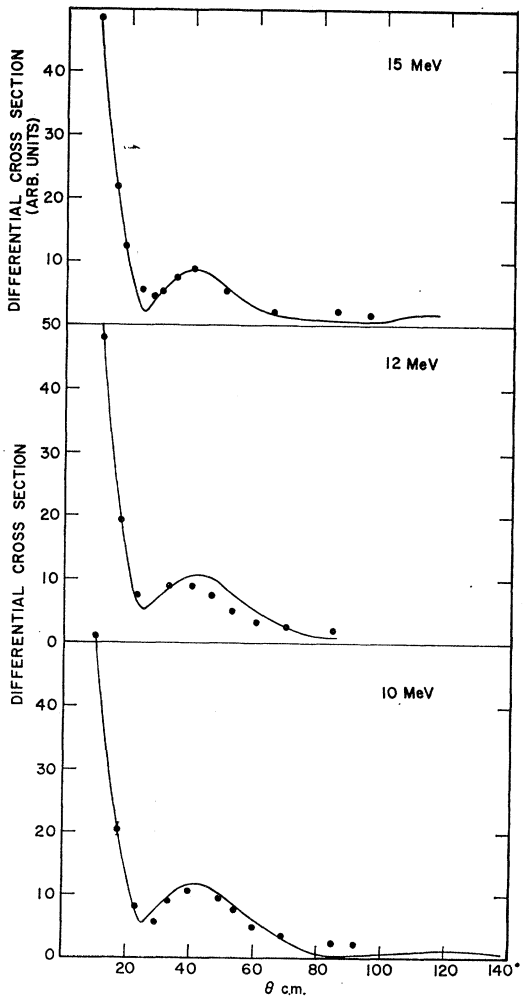

FIG. 8. Calculated and measured angular distributions for reaction $C^{12}(d, p)C^{13*}$ (3.09 MeV). Measurements are from Ref. 5 (10.2 and 12.4 MeV) and Ref. 6 (14.9 MeV). Solid curves are calculated with set B parameters.

show that they depend principally on the proton spin-orbit force.

In Ref. 35, it is shown that, with no spin-orbit term in the neutron potential, P_d and P_y are related by

$$P_d=\tfrac{2}{3}P_y. \tag{13}$$

These quantities are sensitive to the proton parameters in the same way as elastic scattering polarization, to which they are closely related[29–32,34]: For example, the minimum and maximum near 100° in Fig. 7 for the stripping reaction are direct reflections of the corresponding minimum and maximum near 70° in Fig. 1 for elastic scattering. The shift in angle results from the proton energy difference. The proton energy in Fig. 1 is 14.5 MeV; in the stripping reaction with $E_d=10$ MeV the corresponding proton energy $\simeq 9$ MeV.

The averaging over $\mathbf{k}_p$, of the proton scattering which occurs in (1) damps the more prominent structure in the polarization. For the stripping reaction, the maxima and minima in P_y are smaller in magnitude than for the corresponding elastic scattering. At small angles the averaging introduces into the stripping curves structure which is not present in elastic scattering.

2. *Reactions with $l_n\neq 0$*

In this case, the nonspherical neutron capture in the factor (12) contributes to both P_d and P_y as described in Refs. 30–32. This contribution is often dominant, especially near the stripping peak. In Fig. 10, we compare values of P_d and P_y calculated with and without proton spin-orbit force. We also include curves calculated from the "unscattered" amplitude alone. Although the values for P_d and P_y depend on the proton scattering, especially at angles larger than the stripping peak, P_d is insensitive to the proton spin-orbit force for angles out to 140° and P_y out to 40°. In general, P_y depends on the proton spin-orbit force more than P_d.[35]

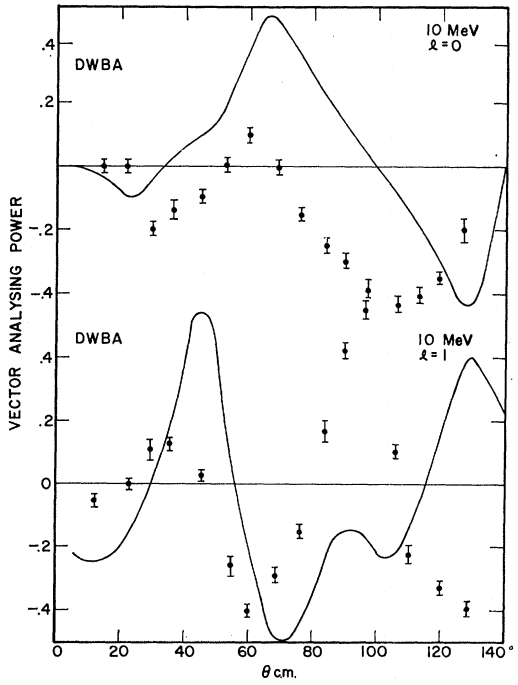

FIG. 9. DWBA calculations of Ref. 22 compared with measured values for P_d for reactions $C^{12}(d, p)C^{13}$ (g.s.), $C^{12}(d, p)C^{13*}$ (3.09 MeV) ($E_d=10$ MeV).

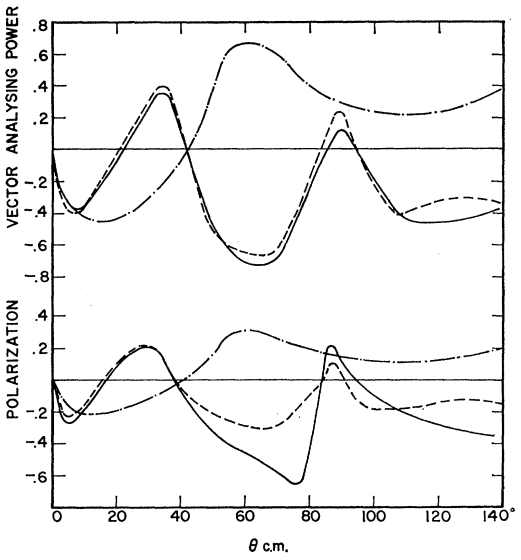

FIG. 10. Comparison of calculated values for P_d, P_y for reaction $C^{12}(d, p)C^{13}$(g.s.) ($E_d=11.9$ MeV). Solid curves are calculated with set A parameters, broken curves with proton spin-orbit force zero, broken dotted curves with "unscattered" amplitude alone.

When the proton spin-orbit force is zero, P_d is simply related to P_y,[35]

$$P_d=2P_y, \tag{14}$$

with the usual limits[38] on absolute magnitudes

$$P_y(\theta)\leq\tfrac{1}{3}, \qquad j_n=l_n-\tfrac{1}{2},$$
$$P_y(\theta)\leq\tfrac{1}{3}l/(l+1), \qquad j_n=l_n+\tfrac{1}{2}. \tag{15}$$

For two similar reactions to final states with $j_n=l_n\pm\frac{1}{2}$ we also find

$$P_d(l_n+\tfrac{1}{2})/P_d(l_n-\tfrac{1}{2})=-l/(l+1). \tag{16}$$

The relations (14)–(16) hold both for the WBP model and the DWBA.

In Fig. 10, the "unscattered" curves, and the predictions without proton spin-orbit force satisfy (14) and (15).

In Fig. 11, we compare calculated and measured

[38] L. B. J. Goldfarb, in *Proceedings of the International Conference on Polarization Phenomena of Nucleons, Karlsruhe, 1965*, edited by P. Huber and H. Schopper (W. Rosch and Co., Bern, 1966), p. 203.

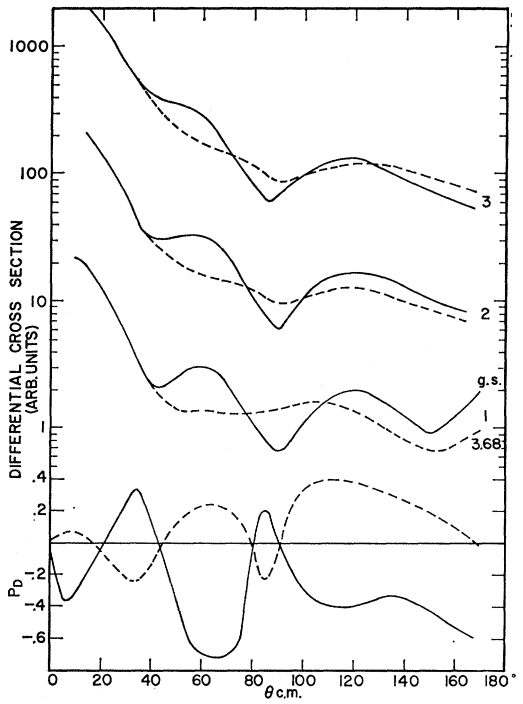

FIG. 11. Differential cross sections and P_d for reactions $C^{12}(d, p)C^{13}$(g.s.), $j=\frac{1}{2}$ (solid curves); $C^{12}(d, p)C^{13*}$ (3.68 MeV), $j_n=\frac{3}{2}$ (broken curves). Lowest pair (1) of differential cross sections is measured values from Ref. 8, center pair (2) is calculated with set A parameters, upper pair (3) with zero proton spin-orbit force. Each pair is normalized to coincide near stripping peak. Values for P_d are also calculated with set A parameters.

angular distributions for reactions $C^{12}(d, p)C^{13}$(g.s., $j_n=\frac{1}{2}$) and $C^{12}(d, p)C^{13*}$(3.68 MeV, $j_n=\frac{3}{2}$). For the two reactions we also compare calculated values for P_d. Angular distributions are calculated from set A parameters with and without proton spin-orbit force curves for P_d include this force.

The calculated values for P_d differ in sign at all angles in agreement with (16). However, the energy difference of 3.68 MeV between the two states precludes detailed quantitative agreement. The proton spin-orbit force has a marked effect on P_d for angles greater than 140°.

The main difference in the shapes of the angular distributions comes from the energy difference between the two states, not from the proton spin-orbit force as in the usual j_n dependence.[30] As for P_d, the proton spin-orbit force has a marked effect only at angles greater than 140°.

Reactions with $l_n=0$ are more sensitive to the details of the proton force, while reactions with $l_n\neq 0$ are sensitive to details of the neutron capture. For a detailed test of the stripping mechanism one thus requires measurements for different angular momentum transfer. Such measurements should also extend to large angles.

B. Anomalies

Certain anomalies appear in the figures shown in Sec. IV. Those for the reaction $C^{12}(d, p)C^{13*}$(3.09 MeV) with $l_n=0$ seem to stem from the proton scattering, those for $C^{12}(d, p)C^{13}$(g.s.) from neutron capture.

In Fig. 1, the calculated and measured elastic scattering polarization differ near 40°, the measured value being more negative. A similar discrepancy in the corresponding stripping curves (Fig. 7) with $l_n=0$, also occurs near 40°. Since P_d and P_y for this reaction reflect the features of the elastic scattering polarization the two anomalies are probably one and the same. This implies that the difficulty is not with the WBP prescription but with the proton optical potential.

The calculated 15-MeV stripping polarization for the same case (Fig. 7) differs from the measured values near 80°. The measurements are poor. However, the discrepancy is particularly interesting since it is difficult for the present form of the WBP model to account for. The calculated values for P_d and P_y which are related by (13) agree with the measurements at lower

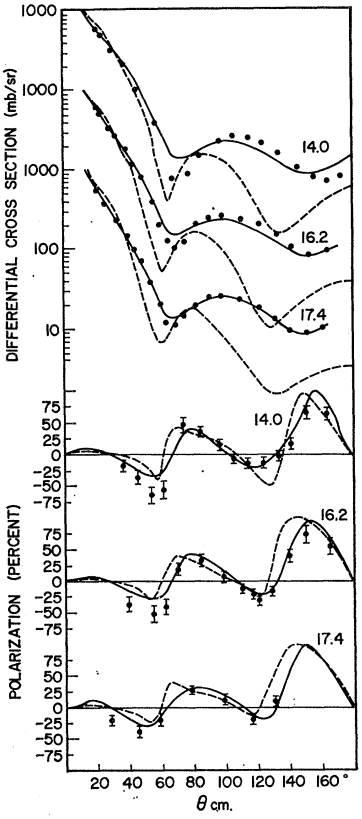

FIG. 12. Differential cross sections and polarization for reaction $C^{12}(p, p)C^{12}$ calculated from Rosen parameters (broken curves) and modified Rosen parameters ($W_p=3$ MeV, $R=1.15A^{1/3}$) (solid curves) compared with differential cross sections (Ref. 40) and polarization (Refs. 41, 42) measured at indicated energies (MeV).

energies. The sudden change is probably not consistent with a simple direct reaction mechanism. It would thus be interesting to measure the corresponding values for P_d at 15 MeV.

In Figs. 2–6, for the reaction $C^{12}(d, p)C^{13}$(g.s.) the calculated and measured values for P_y consistently differ in sign near 30°. The differential cross sections are too large at this angle. With increasing energy the calculated maximum near 80° in both P_d and P_y slips backwards and downwards from the measured points. Improvement in the description of the neutron capture can probably remove all these discrepancies. An energy dependence in the radius or depth of neutron and proton scattering potentials would certainly remove the latter.

Nucleon-nucleus potential which best fit elastic scattering data for individual nuclei may be preferable to the "average" Rosen potentials, especially for light nuclei for which the "average" fits are poor. For protons incident on C^{12} the reaction cross section predicted from the Rosen parameters is several times larger than observed, and the elastic scattering cross section is an order of magnitude too small at backward angles. Both these difficulties can be overcome by lowering the imaginary potential.

In Fig. 12, we compare fits to proton elastic scattering cross sections and polarization using the Rosen potential and a potential differing from it in the parameters $R_p=1.15\ A^{1/3}$, $W_p=3$ MeV. Predicted reaction cross sections at $E_p=10.5$ MeV and $E_p=29$ MeV are 492 and 297 mb, compared with measured values 332 ± 19 and 418 ± 18 mb, and the values 854 and 634 mb, calculated from Rosen parameters.[39–41]

In Figs. 2 and 3, values for P_d, P_y calculated with neutron and proton potentials modified as above are shown for the reaction $C^{12}(d, p)C^{13}$(g.s.) ($E_d=10$ MeV). Comparison with the solid curves calculated with set A parameters show the calculated values are insensitive to the large change in W_n and W_p.

V. CONCLUSION

Preliminary calculations with the WBP model in Secs. III and IV are in qualitative agreement with measurements for the reaction $C^{12}(d, p)C^{13}$ at deuteron energies between 7.0 and 26 MeV. Differences appear to stem from approximations of the present calculations rather than the model itself. In particular no difficulties are associated with the prescription for the proton scattering, so that the basic picture of the WBP model is confirmed.

In the energy range considered, there is no evidence for compound-nucleus resonance effects, except possibly in the reaction $C^{12}(d, p)C^{13*}$(3.09 MeV) at $E_d=15$ MeV, although there may be a small unpolarized energy-dependent background.

The calculations have been made with the average parameters of Rosen *et al.*[33] adjusted to better fit elastic scattering polarization on C^{12}. A detailed parameter search has not been necessary. Comparison of DWBA curves shown in Fig. 9 indicates that careful choice of mechanism is more important than careful choice of parameters.

It is unlikely that fortunate choice of parameters can restore agreement with the DWBA calculations, especially since such calculations depend weakly on spin-orbit forces[22] for angles less than 60°. The failure of DWBA in fitting the data for this reaction appears to stem from an inappropriate description of the reaction mechanism. When interacting with the target nucleus the neutron and proton from the deuteron move under predominantly independent forces and not a force acting on the deuteron center of mass.

ACKNOWLEDGMENTS

We would like to thank Professor W. Haeberli and Dr. T. J. Yule for communicating their data before publication, and Dr. L. C. McIntyre for many helpful discussions.

[39] B. D. Wilkins and G. Igo, Phys. Rev. **129**, 2198 (1963); M. Q. Makino, C. N. Waddell, and R. M. Eisberg, Nucl. Phys. **50**, 145 (1964).

[40] R. W. Peelle, Phys. Rev. **105**, 1311 (1957).

[41] S. Yamabe, M. Kondo, S. Kato, T. Yamazaki, and T. Ruan, J. Phys. Soc. Japan **15**, 2154 (1961); K. W. Brockman, Phys. Rev. **110**, 163 (1958).